Environ. Sci. Technol. **2006**, *40,* 6377−6383

Intercomparison of Thermal and Optical Measurement Methods for Elemental Carbon and Black Carbon at an Urban Location

R. HITZENBERGER,*,† A. PETZOLD,‡ H. BAUER,§ P. CTYROKY,† P. POURESMAEIL,§ L. LASKUS,|| AND H. PUXBAUM§

Institute for Experimental Physics, University of Vienna, Boltzmanng. 5, A-1090 Vienna, Austria, Institut für Physik der Atmosphäre, DLR, Oberpfaffenhofen, Germany, Institute for Chemical Technologies and Analytics, University of Technology of Vienna, Getreidemarkt 8, A-1060 Vienna, Austria, and Umweltbundesamt, Berlin, Germany

Despite intensive efforts during the past 20 years, no generally accepted standard method exists to measure black carbon (BC) or elemental carbon (EC). Data on BC and EC concentrations are method specific and can differ widely (e.g. Schmid et al., 2001, ten Brink et al., 2004). In this study, a comprehensive set of methods (both optical and thermal) is compared. Measurements were performed under urban background conditions in Vienna, Austria, a city heavily impacted by diesel emissions. Filter and impactor samples were taken during 3 weeks in summer 2002 and analyzed for EC with thermal methods: a modified Cachier method (Cachier et al., 1989), a thermal-optical method (Schmid et al., 2001), and the VDI method (VDI, 1996); for BC with optical methods: a filter transmission method and the integrating sphere method (Hitzenberger et al., 1996); and for total carbon (TC) with a combustion method (Puxbaum and Rendl, 1983). The online methods aethalometer (Hansen et al., 1984) and the multiangle absorption photometer MAAP (Petzold et al., 2002) to measure BC were also used. The average values of BC and EC obtained with the methods agreed within their standard deviations. A conversion table was set up to allow comparisons between data measured elsewhere under urban background conditions (with similar source characteristics) with different instruments. An approach to estimate the absorption coefficient from attenuation data is derived so that existing records of aethalometer data in urban environments may be used to obtain also the absorption coefficients.

Introduction

Aerosol black carbon (BC, measured by optical techniques) or elemental carbon (EC, measured by thermal techniques) originates from incomplete combustion of carbonaceous fuel. Recent estimates (*1*) give the total anthropogenic source strength as 8 Tg C/yr (range: 4.3−22 Tg/yr). Although it is a minor component in terms of mass (ca. 5−15% even in areas with a strong traffic source (*40*)), it is important from both climatic and health standpoints. As the main absorber of visible light it causes positive radiative forcing (*2*). Freshly emitted BC or EC from combustion engines is in the ultrafine size range (<100 nm) and is suspected to cause severe health effects (*3*). Setting environmental standards for EC or BC has long been under discussion but not been implemented because of the difficulty of selecting a universally accepted standard technique.

Various measurement methods exist, but intercomparison studies have shown that analysis of identical samples by different methods can result in EC or BC values that differ by up to a factor of 2 (*4*). These results may be caused by effects of the size distribution and mixing state of the aerosol and the presence of other compounds. Methods that compare fairly well for one type of aerosol may disagree for another one.

Most of the BC or EC method intercomparison studies reported so far compare only a limited set of methods. The focus often is on thermal methods (*5*−*8*), optical methods (*9*), or on comparing an optical and a thermal method (*10*−*12*). Some studies were conducted on a limited number of thermal and optical methods (*13*−*15*). In other cases, a specific sample is investigated using a wide range of methods (*4*, *16*), but, in this case, all online methods are excluded a priori. In the INTERCOMP2000 study (*17*), several methods (both thermal and optical) were compared for a European background aerosol, but there is no previous study for urban aerosols.

We therefore focus here on an intercomparison of most methods used in Europe to measure BC or EC under urban background conditions in summer. One goal was to assess available EC and BC methods and to establish conversion tables that enable a better comparison of data obtained with different methods. Optical methods are easy to operate and inexpensive. Unfortunately, they measure BC only via light absorption, so our other goal was to quantify the link between thermal and optical methods. BC mass concentrations are then obtained using conversion factors. Online optical methods (aethalometer, MAAP) are frequently used for air quality monitoring in urban environments. Long-term records of aethalometer data are available for a large number of measurement sites. A method is proposed for estimating the absorption coefficient σ_a from aethalometer attenuation data for urban conditions, as σ_a is more important than total BC concentration for studying the radiative effects of aerosols.

Experimental Section

Vienna (population 1.8 million) is situated in densely populated and heavily industrialized Central Europe, i.e., downwind of other major source areas, so the aerosol in Vienna is usually aged and well mixed with respect to ionic constituents (*18*). Traffic is a major local source of primary particles (*19*). Differences in the size distributions of total carbon (TC) and gravimetric mass indicate a partly external mixture with respect to TC (*20*). In 2002, 70% of fuel sold in Austria was diesel fuel. All heavy duty vehicles and 71% of passenger cars have diesel engines (*21*). Traffic is the largest source of BC in summer, as no space heating is necessary.

Measurements were performed at the roof laboratory (ca. 35 m above ground) of the physics building located in downtown Vienna. A major road passes within 100 m, but the geometry of interconnecting buildings and courtyards shields the site from fresh traffic emissions except those from the street directly below which is used, however, mainly for

* Corresponding author e-mail: regina.hitzenberger@univie.ac.at.
† University of Vienna.
‡ DLR.
§ University of Technology of Vienna.
|| Umweltbundesamt.

10.1021/es051228v CCC: $33.50
Published on Web 09/15/2006

TABLE 1. Description of Methods, Their Codes, Filters, and Other Characteristics

method	code	on/offline	filter type	flow rate (Lpm)	face velocity (m/s)	upper cut size (μm)	wavelength
aethalometer	AET	online	quartz fibre filter tape				"white"/830 nm
light transmission	LTM	offline	Pallflex Tissue Quartz 2500QAT-UP	38	0.4	110	"white"
multiangle absorption photometer	MAAP	online	Glassfibre Schleicher & Schuell GF 10				670 nm
integrating sphere	IS	offline	MSI Polycarbonate, 0.2 μm pore size	7	0.07	106	550 nm
thermooptical	TO	offline	Pallflex Tissue Quartz 2500QAT-UP	38	0.4	110	charring corr.: 632.8 nm
modified cachier	Cachier	offline	Pallflex Tissue Quartz 2500QAT-UP	38	0.4	110	na[a]
Cachier (corrected for carbonates)	EC − IC	offline	Pallflex Tissue Quartz 2500QAT-UP	38	0.4	110	na[a]
VDI 2465/1	VDI	offline	Glassfibre Schleicher & Schuell #10	37	0.39	109	na[a]

[a] na, nonapplicable.

parking. The roof laboratory has an unobstructed fetch for all wind directions except due west, where the Vienna General Hospital buildings create turbulences.

Meteorological Conditions. Meteorological information was obtained from the Zentralanstalt fuer Meteorologie und Geodynamik (ZAMG) situated about 1 km north of the sampling site. Data from these two sites had been found quite comparable previously (Reischl, personal communication).

Samples were collected from June 21 to July 15, 2002. Winds were mainly from westerly directions with variable speed (24 h averages: 2.9−18.3 km/h). There was no precipitation except in short thunder showers. Average humidities ranged from 54.5 to 78.5%. Temperatures were quite high for the site with 24 h averages between 15.2 and 26.6 °C. Long-term monthly averages are 17.7 °C for June and 19.6 °C for July. High temperatures and strong insolation resulted in even higher temperatures in the lab causing data losses due to the malfunction of online instruments during the first days. Forced ventilation subsequently kept laboratory temperatures more or less at ambient levels.

Sampling Schedule. Twenty-four-h filter samples were collected. Sampling started at 14:00 (=12:00 UTC) and continued to 13:45 the next day. The online instruments aethalometer and MAAP sampled continuously. Hourly averages of the online data were calculated. If the standard deviation of an hourly average was > ±50%, the average was rejected. These highly variable online data occurred mainly during the first days (instrument overheating) and during thunderstorms. For the comparison with a 24-h offline sample, only sets of averages containing at least 18 valid hourly averages were used. The data in these sets were averaged and compared to the filter data.

Filter Samples. Filter samples were collected with upside down open face filter holders shielded against precipitation by shrouds threaded over the vacuum lines, which did not disturb the flow conditions unduly. Some losses of large particles (larger than several micrometers) may have occurred, but these losses are negligible for BC and EC.

Total gravimetric mass was measured on the polycarbonate filters used for the BC determination in the integrating sphere method. Prior to weighing, all substrates were conditioned for at least 24 h under 22−27 °C and 41−61% relative humidity. At the higher humitidies, aerosol mass deposits may have been overestimated by about 10% (*22*). The polycarbonate filters were equilibrated within the weighing chamber of the microbalance (Mettler ME3) for 8 min in the presence of an ion source before weighing. Under these conditions, errors could be kept within ±3 μg.

Methods for Carbon Determination. Table 1 gives an overview of the methods and the codes we assigned for easier method identification in tables and figures.

Optical Methods. Four optical methods for BC analysis were used. The aethalometer (*23*) (Magee Scientific AE-9) and the light transmission method (*24*) use light transmission measurements. The transmission of a loaded filter for "white" light or light in a specified wavelength band (see Table 1) is measured and compared to the transmission of a clean filter either online (aethalometer) or offline (light transmission method). The decrease in light transmission (i.e. the attenuation $ATN = \ln(T/T_0)$, with T and T_0 the transmission of the loaded and clean filter, respectively) can be taken as a measure of the aerosol absorption coefficient σ_a. BC concentrations are calculated from σ_a with method specific conversion factors.

As was demonstrated for both ambient (*25*−*27*) and laboratory test aerosols (*28*−*30*) all filter-transmission (and reflectance) methods must be corrected for light scattering effects (scattering by particles and multiple scattering by the filter matrix) to obtain a reliable measurement of σ_a. The BC mass may then be calculated from the corrected σ_a using a mass absorption coefficient. For the aethalometer, however, it is common practice to use a conversion factor of 19 m^2/g (*31*) to obtain BC mass directly from the filter attenuation ATN. We followed the same procedure also for the light transmission method, although the conversion factor for aethalometer and LTM-type methods is still under debate. Reported values range from <10−14 m^2/g (*27*, *27*) to 25 m^2/g (*32*). The reason for this strong variation of conversion factors is not yet known. Attempts to correct for influences of light-scattering aerosol components and the filter matrix were made (e.g. refs *28* and *30*), but no sufficient solution was found. We therefore decided to use the conversion factor of 19 m^2/g which is recommended by the manufacturer. A different conversion factor X can easily be applied by multiplication of aethalometer data with the ratio of 19/X.

Multiangle absorption photometry (MAAP) is based on simultaneous measurements of radiation transmitted through and scattered back from a particle-loaded fiber filter (*33*, *34*). Irradiation measurements at several detection angles permit the full determination of the radiation fields in the forward and back hemispheres. The absorption coefficient σ_a of the deposited aerosol is calculated using radiative transfer techniques. Intensive calibration and intercomparison studies using light-absorbing and light-scattering particles (*29*, *35*) showed that σ_a values measured by the MAAP at $\lambda = 670$ nm are in close agreement with σ_a measured by in situ techniques (photoacoustic spectrometry; extinction plus scattering coefficient measurements). The differences between in situ and MAAP-derived σ_a are below 5%. A conversion factor of 6.5 m^2/g at $\lambda = 670$ nm was used (*34*) to obtain BC concentrations from σ_a measured with the MAAP.

For the integrating sphere method (*36*) liquid suspensions of BC are produced by dissolving the loaded sampling

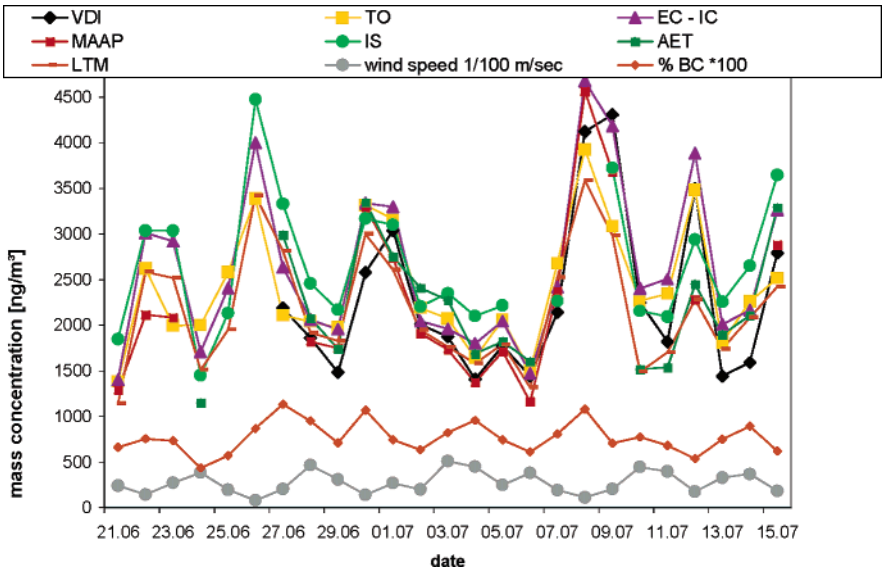

FIGURE 1. All EC and BC mass concentrations obtained from the filter based and continuous sampling techniques (method codes in Table 1).

substrate in a suitable solvent (chloroform for polycarbonate filters). The signal decrease caused by BC is converted to BC concentration using a calibration curve obtained with a commercial carbon black (Elftex 124, Cabot Corporation). As the refractive index of the solvents is similar to that of most aerosol material, no enhanced light absorption occurs even if some of this material is not dissolved.

Thermal and Thermooptical Methods. Elemental carbon (EC) was analyzed on filter samples using a two-step combustion method (*37*). Filters were heated for 2 h at 340 °C in an oxygen atmosphere to remove organic carbon (OC). In a subsequent high-temperature step (1000 °C, O_2), EC (and carbonate carbon, IC) is oxidized. CO_2 originating in this step is detected by a NDIR analyzer (*38*). In the original Cachier method (*37*), carbonates are removed by exposing the filters to HCl. In our study, a different correction for carbonates was performed by subtracting the carbonates obtained with the thermooptical method (see below) from the EC values. The carbonate-corrected values are labeled EC-IC. Because the exposure to HCl was not performed, the two-step combustion method therefore is called "modified Cachier method" in this study.

As some organic material pyrolyzes during the low-temperature oxidation step, charring corrections were developed for several methods. In the thermooptical method (*4*), samples are heated continuously ($\Delta T = 20$ °C/min) to a final temperature of 800 °C in pure O_2. A MnO_2 catalyst (at 700 °C) converts all the evolved carbonaceous gases to CO_2, which is detected by a NDIR detector. Throughout the process, the filter transmission is monitored using a HeNe laser beam and a photodetector. During heating, the light transmission decreases to a minimum. The first peak in CO_2 that evolves after the transmission has reached again the initial value is assigned to EC. Carbonate carbon causes another distinct peak which evolves after the EC peak at ca. 600 °C.

In the VDI 2465/1 method (*39*), extractable OC is analyzed by placing the filters for 24 h in a 50:50 mixture of toluene and 2-propanol. The filters are then dried and heated for 1 min at 200 °C and for 7 min at 500 °C. Carbon evolving from the filters in this step is assigned to nonextractable OC. EC is then determined by combustion at 650 °C in an O_2 atmosphere. The minimum detectable carbon mass loading is 9 μg C.

Results

Figure 1 shows all carbon data together with wind speed as an indicator for the meteorological situation. The first data point corresponds to the sample starting on Friday, June 21, 2002 at 14:00. Concentrations range from 1000 to approximately 5000 ng m^{-3} which covers a representative range of values for an urban Central European atmosphere in summer (*40*). The data all follow the same trend and are quite well correlated. A trend of high concentrations under conditions of low wind speeds is visible. The variation of % BC (of total gravimetric mass; IS data), however, is not linked to wind speed (which causes dilution effects). The BC content of the aerosol varied between 4.3 and 11.3%, with an average value of 7.7% (±1.7%; IS data).

Absorption Coefficients Obtained from Optical Methods. The MAAP provides σ_a without further need for data correction, as was demonstrated in various intercomparison experiments (*29*, *35*). The aethalometer gives an attenuation coefficient σ_{ATN} which has to be converted into σ_a by correcting for light scattering effects caused by the aerosol constituents and the filter matrix. No generally accepted correction function is available, which would permit the calculation of σ_a from ATN. In a laboratory study (*28*), a conversion of σ_{ATN} to σ_a via

$$\sigma_a = \frac{\sigma_{ATN}}{C \cdot R(ATN)}$$

was proposed. C is an empirical factor which accounts for enhanced light attenuation in an unloaded filter (caused by multiple scattering by the filter fibers), while the function R(ATN) reflects the effect of light scattering by aerosol particles. The factor C is determined from the filter attenuation at an attenuation value of 10%, $\sigma_{ATN\ 10\%}$, normalized to the "true" absorption coefficient σ_a determined from the MAAP data; i.e., $C = \sigma_{ATN\ 10\%}/\sigma_a$. From our data set, we obtain $C = 3.94 \pm 0.89$, which is close to the $C = 3.90 \pm 1.13$ reported for coated diesel soot particles (*28*).

The aerosol absorption coefficients were calculated from the 24 h-averaged aethalometer data assuming that the spectral distribution of the broad-band light source in the AE-9 instrument peaks at a wavelength of 830 nm (*31*). Assuming a λ^{-1} dependence of σ_a, the aethalometer data were corrected for the MAAP operation wavelength of 670 nm. The average ratio of absorption coefficients estimated from

TABLE 2. Daily Averaged Data for the Absorption Coefficient σ_a and Mass Specific Absorption Coefficient B_a at $\lambda = 630$ nm[a]

	σ_a Mm^{-1}		B_a (BC) m^2 g^{-1}		
date	MAAP[b]	AET[b]	EC (TO)[b]	EC - IC[b]	EC (VDI)[b]
21. Jun	8.5		6.16	6.06	
22. Jun	14.0		5.33	4.63	
23. Jun	13.7		6.88	4.71	
24. Jun		6.6			
25. Jun					
26. Jun					
27. Jun		17.2			
28. Jun	12.0	11.9	5.91	5.84	6.48
29. Jun	11.5	10.0	5.83	5.89	7.78
30. Jun	21.7	19.3	6.56	6.51	8.43
01. Jul	18.0	15.8	5.70	5.47	5.93
02. Jul	12.6	13.9	5.76	6.17	6.28
03. Jul	11.5	13.1	5.53	5.84	6.13
04. Jul	9.1	9.7	5.52	5.03	6.42
05. Jul	11.3	10.5	5.49	5.53	6.39
06. Jul	7.7	9.2	5.12	5.24	5.34
07. Jul	15.7		5.85	6.48	7.32
08. Jul	30.1		7.68	6.45	7.31
09. Jul	24.3		7.87	5.80	5.63
10. Jul		8.8			
11. Jul		8.9			
12. Jul	15.0	14.1	4.32	3.88	4.30
13. Jul		10.9			
14. Jul		12.1			

[a] For the calculation of B_a, σ_a obtained with the MAAP was divided by the EC concentration obtained from various methods. [b] Method.

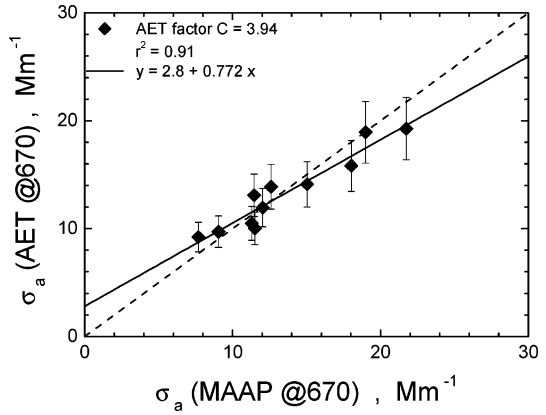

FIGURE 2. Comparison of aerosol light absorption coefficients obtained from attenuation data (AET) with the absorption coefficients measured by multiangle absorption photometry (MAAP); solid and dashed lines indicate linear regression and 1:1 relationships.

wavelength-corrected attenuation data ($\sigma_{a\,AET}$) and determined by the MAAP instrument ($\sigma_{a\,MAAP}$) is $\sigma_{a\,AET}/\sigma_{a\,MAAP} = 1.00 \pm 0.12$. For 1 h-averaged data this ratio is 1.02 ± 0.30. In our simplified approach, the effect of light scattering aerosol components is neglected, i.e., $R(ATN) = 1.0$. The correction for the enhanced light scattering in the filter matrix permits an estimate of σ_a from attenuation data within an uncertainty of ±25% for 95% statistical significance or ± 2 × standard deviation, respectively.

The σ_a measured by the MAAP and estimated from attenuation data are compiled in Table 2 for the entire study and shown in Figure 2. The results of the linear regression analysis performed on these data are summarized in Table 3. Table 3 also contains aethalometer data corrected for the wavelength shift from 830 nm (aethalometer peak wavelength) to 670 nm (MAAP operation wavelength). The offset of attenuation data to MAAP data in Figure 2 can be attributed to the fact that σ_a was estimated from attenuation data by a simple method which does not account for the full physics behind the processes of light scattering and absorption by particles embedded in a fibrous filter matrix. Neglecting the effect of light scattering in the estimation approach may explain the positive σ_a value estimated from attenuation data, while the MAAP method gives $\sigma_a = 0$. Nevertheless, on average the absorption coefficient σ_a AET from the corrected attenuation data is in close agreement with $\sigma_{a\,MAAP}$, see Table 3. The estimation method therefore offers a possibility for calculating σ_a from existing aethalometer data records.

The mass-specific absorption coefficients B_a(BC) were determined by dividing the $\sigma_{a\,MAAP}$ (at 670 nm wavelength) by the EC mass concentrations obtained from the thermal methods. B_a is widely used for the conversion of σ_a data into BC mass concentrations for both experimental observations and theoretical calculations. The results from the linear regression analyses are summarized in Table 3. Converting the slopes of regression lines to a wavelength of 550 nm, we found a range of values of B_a(BC) from 6.8 to 8.7 m^2/g, which is in good agreement with B_a(BC, 0.55 μm) ≤7.5 m^2 g^{-1} for spherical carbonaceous particles and <10 m^2 g^{-1} for internally mixed atmospheric BC (*41*). A recent review (*42*) recommended $B_a = 8$ m^2/g at 550 nm which agrees excellently with our results.

Comparison of EC and BC Concentrations. As no reference method exists for the determination of EC or BC, we calculated the campaign average concentration and its standard deviation for each method separately (Figure 3). Comparing all data to the last bar, which corresponds to the average of all averages, agreement is very good. The IS method (filter samples) gave the highest concentration (ratio to average: 1.120 ± 0.115), followed by the modified Cachier method (1.083 ± 0.083), the thermooptical method (1.019 ± 0.122), the aethalometer (0.979 ± 0.138), the VDI method (0.935 ± 0.126), the MAAP (0.911 ± 0.090), and the LTM (0.910 ± 0.082). The average values of BC and EC agree within their standard deviations, so none of the methods is completely unacceptable for air quality monitoring purposes.

Correlations between the Methods. To compare the methods with each other, we performed a linear regression analysis of all methods (Table 4). Such a regression approach is often used in method comparisons, but as no standard method exists, the choice of "reference" method (i.e. the one on the *x*-axis) is arbitrary. The parameter on the *x*-axis should be free of statistical error, which is an unreasonable assumption. Despite these reservations, we performed the regression analysis so that our study can be compared to others using this approach.

As can be seen from Table 4, several of the regression coefficients (given here in terms of r^2) are not significant. The best correlations were found among the optical and the thermal and thermooptical groups. The worst correlations were found between the aethalometer and the thermal and thermooptical methods. Examples of regression plots are given in Supporting Information S1 for the optical methods against the MAAP and S2 for all methods vs the carbonate-corrected Cachier method.

Tables 4 and 5 show sets for conversion factors for all methods we used. Table 4 contains the parameters of the linear regression, and Table 5 contains the average ratios between data obtained with different methods. Since the linear regression line should ideally have a zero *y*-axis intercept, the slope and the method ratio should agree within the limits of uncertainty.

The tables should not, however, be taken as general tables for data conversion for all possible sites, aerosol types, sources, and composition. Apart from differences in methodology, EC or BC concentrations derived from different methods are also sensitive to aerosol size distribution, mixing

TABLE 3. Linear Regression Analysis for Methods AET vs MAAP as the Absorption Coefficient Reference Method ($\sigma_{a\ Method} = a + m \times \sigma_{a\ MAAP}$) and Linear Regression Analysis of σ_{ap} Measured with the MAAP vs EC Mass Concentration ($\sigma_{a\ MAAP} = a + m \times B_a \times c_{EC\ Method}$)[a]

	σ_a, Mm^{-1}		B_a, m^2 g^{-1}		
	AET (830 nm)[b]	AET (670 nm) $C = 3.94$[b]	EC (TO)[b]	EC - IC[b]	EC (VDI)[b]
N	10	10	16	16	13
r^2	0.910	0.910	0.776	0.834	0.778
a	9.32 (3.79)	2.82 (1.15)	−2.54 (2.54)	−0.03 (1.84)	1.62 (2.32)
m	2.55 (0.27)	0.77 (0.08)	7.18 (0.99)	5.61 (0.65)	5.74 (0.88)

[a] The uncertainties of the values are given as standard deviations in parentheses. [b] Method.

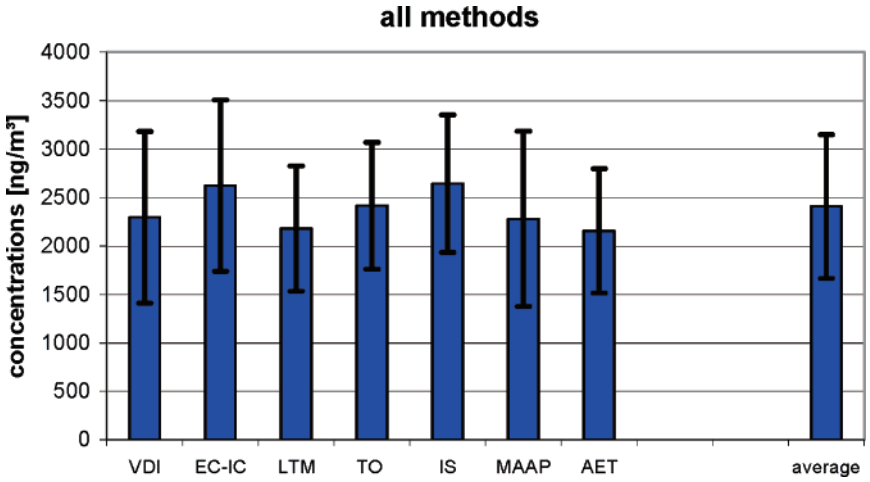

FIGURE 3. Average mass concentrations of EC and BC obtained with the different methods for the whole measurement campaign. The error bars correspond to the standard deviations of the campaign averages.

TABLE 4. Parameters of the Regression Lines for All Data[a]

X/Y	TO	VDI	EC - IC	MAAP	LTM	AET	IS
TO		1.1824	1.2399	1.0876	0.822	0.7099	0.8306
		−594.03	−373	−383.79	+194.56	+537.68	+658.71
		0.7774	0.8471	0.7766	0.691	0.3771	0.4485
VDI	0.6575		0.965	0.8695	0.5444	0.6373	0.5535
	+934.39		+422.08	+244.73	+928.13	+902.45	+1398.2
	0.7774		0.9281	0.7788	0.6282	0.4313	0.6043
EC - IC	0.6832	0.9618		0.8495	0.6514	0.6778	0.7938
	+624.16	−240.9		−4.9945	+472.12	+539.19	+593.1
	0.8471	0.9281		0.8341	0.7876	0.5121	0.7482
MAAP	0.7141	0.8956	0.9818		0.669	0.885	0.7457
	+821.16	+323.08	+451.21		+698.06	+490.74	+1042.5
	0.7766	0.7788	0.8341		0.8799	0.9101	0.7573
LTM	0.8407	1.1539	1.2091	1.3152		1.2158	1.1031
	+582.82	−217.59	−13.766	−644.28		−260.84	+264.88
	0.691	0.6282	0.7876	0.8799		0.8354	0.8072
AET	0.5312	0.6767	0.7555	1.0284	0.6871		0.8254
	+1134.1	+563.61	+756.1	−319.49	+506.39		+710.71
	0.3771	0.4313	0.5121	0.9101	0.8354		0.8659
IS	0.5399	1.0917	0.9426	1.0155	0.7317	1.0491	
	+962.31	−640.68	+91.295	−524.32	+221.97	−451.96	
	0.4485	0.6043	0.7482	0.7573	0.8072	0.8659	

[a] In each cell, the first line corresponds to the slope of the regression line, the second corresponds to the intercept, and the third one gives the regression parameter r^2. For the method codes, see Table 1.

state, and chemical composition (inorganic substances and carbonacous material). The factors we give here were obtained under summer conditions in an urban background aerosol without direct impact from traffic and other combustion sources but in a country with a high percentage of diesel cars. At street level, e.g., the conversion factors could be quite different. An earlier comparison between an aethalometer and the IS method on aerosol sampled at sidewalk level in June 1998 in Vienna showed that the aethalometer gave only about 50% of the BC measured with the IS method, even though the same IS and calibration curve had been used (Hitzenberger, private communication). In the data set obtained at roof level, the aethalometer data are quite comparable to the IS data (the aethalometer gives 86% of the BC measured with the IS). In a future study a similar intercomparison will be performed for winter conditions in order to extend the method assessment for BC measurement methods.

TABLE 5. Campaign Averages of the Ratios of Mass Concentrations Obtained by the Method Given in the Top Line to the Mass Concentrations Obtained by the Method Given in the Left Column[a]

	VDI	EC - IC	LTM	TO	IS	MAAP	AET
VDI		1.171	0.995	1.109	1.239	0.980	1.103
		0.131	0.204	0.173	0.248	0.159	0.216
EC - IC	0.864		0.848	0.945	1.043	0.850	0.918
	0.094		0.117	0.120	0.152	0.109	0.186
LTM	1.050	1.204		1.131	1.238	1.008	1.077
	0.237	0.185		0.183	0.160	0.136	0.143
TO	0.925	1.076	0.907		1.122	0.919	0.957
	0.161	0.149	0.153		0.230	0.146	0.225
IS	0.840	0.979	0.821	0.928		0.812	0.861
	0.177	0.149	0.111	0.195		0.127	0.105
MAAP	1.048	1.198	1.008	1.114	1.258		1.147
	0.187	0.179	0.131	0.173	0.182		0.130
AET	0.948	1.139	0.945	1.106	1.177	0.882	
	0.232	0.265	0.135	0.283	0.134	0.097	

[a] As the average of the ratios of method 1 and method 2 is not equal to the inverse of the average of the ratios of method 2 and method 1, the table is not symmetrical.

Acknowledgments

The authors would like to thank H. Giebl of the Institute for Experimental Physics for helping with changing filters and R. Ellinger for providing the aethalometer. The development of the integrating sphere method was funded by the Hochschuljubiläumstiftung der Stadt Wien, H 85/92.

Supporting Information Available

BC concentrations obtained by the optical methods vs the BC concentrations measured with the MAAP instrument (S1) and EC and BC concentrations measured by all methods compared to EC obtained from the carbonate corrected modified Cachier method (S2). This material is available free of charge via the Internet at http://pubs.acs.org.

Literature Cited

(1) Bond, T. C.; Streets, D. G.; Yarber, K. F.; Nelson, S. M.; Woo, J.-H.; Klimont, Z. A technology based inventory of black and organic carbon emissions from combustion. *J. Geophys. Res.* **2004**, *109*, D14203.

(2) IPCC 2001. *Climate Change 2001: The Scientific Basis*; Houghton, J. T., Ding, Y., Griggs, D. J., Noguer, M., van der Linden, P. J., Xiaosu, D., Eds.; Cambridge University Press: U.K.

(3) Kim, H. J.; Liu, X. D.; Kobayashi, T.; Kohyama, T.; Wen, F. Q.; Romberger, D. J.; Conner, H.; Gilmour, P. S.; Donaldson, K.; MacNee, W.; Rennard, S. I. Ultrafine carbon black particles inhibit human lung fibroblast-mediated collagen gel contraction. *Am. J. Respir. Cell Mol. Biol.* **2003**, *28*, 111−121.

(4) Schmid, H. et al. Results of the "carbon conference" international aerosol carbon round robin test stage I. *Atmos Environ.* **2001**, *35*, 2111−2121

(5) Birch, M. E. Analysis of carbonaceous aerosols: interlaboratory comparison. *Analyst* **1998**, *123*, 851−857.

(6) Sciare, J.; Cachier, H.; Oikonomou, K.; Ausset, P.; Sarda-Esteve, R.; Mihalopoulos, N. Characterization of carbonaceous aerosols during the MINOS campaign in Crete, July-August 2001: a multi-analytical approach. *Atmos. Chem. Phys.* **2003**, *3*, 1743−1757.

(7) Chow, J. C.; Watson, J. G.; Chen, L. W. A.; Arnott, W. P.; Moosmuller, H. Equivalence of elemental carbon by thermal/optical reflectance and transmittance with different temperature protocols. *Environ. Sci. Technol.* **2004**, *38*, 4414−4422.

(8) Schauer, J. J. et al. ACE-Asia intercomparison of a thermal-optical method for the determination of particle-phase organic and elemental carbon. *Environ. Sci. Technol.* **2001**, *37*, 993−1001.

(9) Sheridan, P. J.; Arnott, W. P.; Ogren, J. A.; Andrews, E.; Atkinson, D. B.; Covert, D. S.; Moosmuller, H.; Petzold, A.; Schmid, B.; Strawa, A. W.; Varma, R.; Virkkula, A. The Reno Aerosol Optics Study: An evaluation of aerosol absorption measurement methods. *Aerosol Sci. Technol.* **2005**, *39*, 1−16.

(10) Nejedly, Z.; Campbell, J. L.; Brook, J.; Vet, R.; Eldred, R. Evaluation of elemental and black carbon measurements from the GAViM and IMPROVE networks. *Aerosol Sci Technol.* **2003**, *37*, 96−108.

(11) Rice, J. Comparison of integrated filter and automated carbon aerosol measurements at Research Triangle Park, North Carolina. *Aerosol Sci. Technol.* **2004**, *38*, S2, 23−36.

(12) Petzold, A.; Niessner, R. Method intercomparison on soot-selective techniques. *Mikrochim. Acta* **1995**, *117*, 215−237.

(13) Hering, S. V. et al. Comparison of sampling methods for carbonaceous aerosols in ambient air. *Aerosol Sci. Technol.* **1990**, *12*, 200−213.

(14) Hitzenberger, R.; Jennings, S. G.; Larson, S. M.; Dillner, A.; Cachier, H.; Galambos, Z.; Spain, T. G. Intercomparison of measurement methods for black carbon aerosols. *Atmos. Environ.* **1999**, *33*, 2823−2833

(15) Saathoff, H.; Moehler, O.; Schurath, U.; Kamm, S.; Dippel, B.; Mihelcic, D. The AIDA soot aerosol characterisation campaign 1999. *J. Aerosol Sci.* **2003**, *34*, 1277−1296.

(16) Currie, L. A. et al. A critical evaluation of interlaboratory data on total, elemental and isotopic carbon in the carbonaceous particles reference material, NIST SRM 1649a. *J. Res. Natl. Inst. Stand. Technol.* **2002**, *107*, 279−298.

(17) ten Brink, H.; Maenhaut, W.; Hitzenberger, R.; Gnauk, T.; Spindler, G.; Even, A.; Mueller, K.; Tursic, J.; Putaud, J.-P-. Chi, X.; Berner, A.; Bauer, H.; Puxbaum, H. INTERCOMP 2000: the comparability of methods in use in Europe for measuring the carbon content of aerosol. *Atmos. Environ.* **2004**, *38*, 6507−6519.

(18) Okada, K.; Hitzenberger, R. Mixing properties of individual submicrometer aerosol particles in Vienna. *Atmos. Environ.* **2001**, *35*, 5617−5628.

(19) Hitzenberger, R. Absorption coefficients and mass concentrations of the urban aerosol of Vienna, Austria, during the years 1985 and 1986. *Water, Air, Soil Pollut.* **1993a**, *71*, 131−153.

(20) Hitzenberger R.; Puxbaum H. Comparisons of the measured and calculated specific absorption coefficient for Vienna urban aerosol samples. *Aerosol Sci. Technol.* **1993**, *18*, 323−245.

(21) OAMTC Oesterreichischer Automobil und Touring Club, news release, 2004.

(22) Hitzenberger, H.; Dusek, U.; Berner, A.; Alabashi, R. Humidity-dependent growth of size-segregated aerosol samples. *Aerosol Sci. Technol.* **1997**, *27*, 116−130.

(23) Hansen, A. D. A.; Rosen, H.; Novakov, T. The aethalometer − an instrument for the real-time measurement of optical absorption by aerosol particles. *Sci. Total Environ.* **1984**, *36*, 191−196.

(24) Rosen, H.; Novakov, T. Optical transmission through aerosol deposits on diffusely reflecting filters: a method for measuring the absorbing component of aerosol particles. *Appl. Opt.* **1983**, *22*, 1265−1267.

(25) Hitzenberger, R. Absorption measurements with an integrating plate photometer − calibration and error analysis. *Aerosol Sci. Technol.* **1993**, *18*, 70−84

(26) Liousse, C.; Cachier, H.; Jennings, S. G. Optical and thermal measurements of black carbon aerosol content in different environments: variation of the specific attenuation cross-section, sigma (σ). *Atmos. Environ.* **1993**, *27A*, 1203−1211.

(27) Petzold, A.; Kopp, C.; Niessner, R. The dependence of the specific attenuation cross-section on black carbon mass fraction and particle size. *Atmos. Environ.* **1997**, *31*, 661−672.

(28) Weingartner, E.; Saathoff, H.; Schnaiter, M.; Streit, N.; Bitnar, B.; Baltensperger, U. Absorption of light by soot particles: Determination of the absorption coefficient by means of aethalometers, *J. Aerosol Sci.* **2003**, *34*, 1445−1463.

(29) Petzold, A.; Schloesser, H.; Sheridan, P. J.; Arnott, W. P.; Ogren, J. A.; Virkkula, A. Evaluation of multi-angle absorption photometry for measuring aerosol light absorption. *Aerosol Sci. Technol.* **2005**, *39*, 40−51, 2005.

(30) Arnott, W. P.; Hamasha, K.; Moosmüller, H.; Sheridan, P. J.; Ogren, J. A. Towards aerosol light absorption measurements with a 7-wavelength aethalometer: Evaluation with a photoacoustic instrument and 3-wavelength nephleometer. *Aerosol Sci. Technol.* **2005**, *39*, 17−29.

(31) Bodhaine, B. A. Aerosol absorption measurements at Barrow, Mauna Loa and the South Pole. *J. Geophys. Res.* **1995**, *100*, 8967−8975.

(32) Gundel, L. A.; Dodd, R. L.; Rosen, H.; Novakov, T. The relationship between optical attenuation and black carbon concentration for ambient and source particles. *Sci. Total Environ.* **1984**, *36*, 197−202.

(33) Petzold, A.; Kramer, H.; Schönlinner, M. Continuous measurement of atmospheric black carbon using a multi-angle absorption photometer. *Environ. Sci. Pollut. Res.* **2002**, *Special issue 4*, 78−82.
(34) Petzold, A.; Schönlinner, M. Multi-angle absorption photometry − a new method for the measurement of aerosol light absorption and atmospheric black carbon. *J. Aerosol Sci.* **2004**, *35*, 421−441, 2004.
(35) Schnaiter, M.; Schmid, O.; Petzold, A.; Fritzsche, L.; Klein, K.-F.; Andreae, M. O.; Helas, G.; Thielmann, A.; Gimmler, M.; Möhler, O.; Linke, C.; Schurath, U. Measurement of wavelength-resolved light absorption by aerosols utilizing a UV-Vis extinction cell. *Aerosol Sci. Technol.* **2005**, *36*, 249−260.
(36) Hitzenberger, R.; Dusek, U.; Berner, A. Black carbon measurements using an integrating sphere technique. *J. Geophys. Res.* **1996**, *101*, D14, 19601−19606.
(37) Cachier, H.; Bremond, M. P.; Buat-Ménard, P. Determination of atmospheric soot carbon with a simple thermal method. *Tellus 41B* **1989**, 379−390
(38) Puxbaum, H.; Rendl, J. Ein automatisches Analysatorsystem zur Bestimmung von Kohlenstoff und Schwefel in luftgetragenen Stäuben. *Microchim. Acta I* **1983**, 263−272.
(39) VDI 2465 Part 1, 1996. Measurement of soot (Immission) Chemical Analysis of Elemental Carbon by Extraction and Thermal Desorption of Organic Carbon. VDI/DIN-Handbuch Reinhaltung der Luft 4.
(40) Schaap, M.; Denier Van Der Gon, H. A. C.; Dentener, F. J.; Visschedijk, A. J. H.; Van Loon, M.; ten Brink, H. M.; Putaud, J.-P.; Guillaume, B.; Liousse, C.; Builtjes, P. J. H. Anthropogenic black carbon and fine aerosol distribution over Europe. *J. Geophys. Res.* **2004**, *109*, D18207.
(41) Fuller, K.; Malm, W. C.; Kreidenweis, S. M. Effects of mixing on extinction by carbonaceous particles. *J. Geophys. Res.* **1999**, *104*, 15941−15954.
(42) Bond, T. C.; Bergstrom, R. W. Light absorption by carbonaceous particles: An investigative review. *Aerosol Sci. Technol.* **2006**, *40*, 27−67.

Received for review June 27, 2005. Revised manuscript received June 14, 2006. Accepted July 5, 2006.

ES051228V